Available online at www.sciencedirect.com
SCIENCE DIRECT
Catalysis Today 106 (2005) 77–83
CATALYSIS TODAY
www.elsevier.com/locate/cattod

DC and FCC dry gas valorization on PtZrGa/MCM-41

Roberto Galiasso Tailleur *, Jose Bonilla Platin

Simon Bolivar University, Department of Thermodynamics, Sartenejas, Baruta, Venezuela

Abstract

The light olefins present in DC and FCC dry gas can be valorized into aromatics and paraffins. A new PtZrGa/MCM-41 catalyst has been synthetized and used to carry out dimerization and trimerization reactions of olefins. The catalyst was characterized by XRD and using FTIR, XPS, ^{71}Ga and ^{1}H NMR spectroscopies. A blend of ethylene–propylene in presence of CS_2, hydrogen and benzene were tested in a semi-batch-type reactor. A simplified set of reaction is proposed and the operating variables were explored to study the catalytic activity and selectivity. The paper discusses the catalytic surface composition and the sensitivity of the reactions to temperature, hydrogen partial pressure and ethylene/propylene ratio. The catalyst deactivation was analyzed and the industrial implication was discussed.

Keywords: Olefins oligomerization; PtZrGa/MCM-41 catalyst; Kinetics; Aromatics and cyclo-paraffins production

1. Introduction

The stringent US and EU regulation for environmental protection has resulted in the need for new fuels and new ways to valorize refinery streams. The light olefins produced from fluid catalytic crackers and coking units have traditionally been considered low-value by-products and used as fuel gas. Its valorization is hard to be achieved due to its low olefins concentration and the presence of diolefins and sulfur that deactivated the existing catalyst. However, by employing the adequate catalyst, the production of alkylated and oxygenates can be done to produce a high-value gasoline blending components or petrochemical products. The traditional polymerization into alfa-olefins [1,2] required pure olefins. Over the past 20 years, substantial improvements have been made in the design of transition and noble metal catalyst for industrial purposes, especially with the development of metallocenes.

Another useful alternative is the oligomerization of olefins and paraffins into aromatics and cycloalkanes as it was proposed by us [3]. Most of the heterogeneous dimerization–oligomerization technology depends on the catalyst stability due to the high tendency of zeolites to produce coke [4]. MFI-type Ga-silicate has been reported to have an excellent activity in aromatization of propane and butane [5,6] to produce aromatics. Mesoporous silicate like MCM-41, fully patented by Mobil [7], gave the possibility of a selective conversion into bulky-type molecules, with low diffusion control and with particular shape-oriented reactions in the zeolite cages.

This work was focused on studying olefin dimerization and trimerization reactions to valorize a DC and FCC dry gas that contains small amounts of light olefins, diolefins, hydrogen and sulfur compound. The catalyst used was a PtGaZr/MCM-41, a large pore-type zeolite.

2. Experimental

2.1. Catalyst preparation

The catalyst was prepared in Teflon-lined autoclave according to Ref. [8], by blending an aqueous solution of tetramethyl-ammonium silicate (TMAOH-Degussa with 25% concentration and containing 12% of SiO_2) with another aqueous solution of hexadecyl-trimethyl-ammonium hydroxide (CTABr) from Merck. When the solution

* Corresponding author. Present address: ITQ, UPV, 46012 Valencia, Spain.
E-mail address: gatairo@itq.upv.es (R.G. Tailleur).

0920-5861/$ – see front matter © 2005 Elsevier B.V. All rights reserved.
doi:10.1016/j.cattod.2005.07.161

was well homogenized at room temperature, the aqueous zirconium iso-propoxide (Alfa, aqueous solution at 32%) and those of gallium acethyl-acetonate (Aldrich, aqueous solution at 12%) were added under high stirring rate during 2 h. The reactor was then heated to 130 °C using a 20 °C/m ramp of temperature and then maintained at that temperature for 20 h under nitrogen flow. After that, the slurry that formed was filtered and the solid was washed with three portions of methylamine and then with ethanol. The solid was dried in nitrogen at 120 °C for 3 h (mentioned later as the pre-calcinated sample) or in air for 3 h at 200, then at 300 and finally, at 500 °C (named the calcinated sample). The resulting solid was impregnated with an aqueous solution of Pt diamine-chloride compound (Aldrich) at room temperature and subsequently washed, filtered, dried in air at 120 °C for 3 h and then at 500 °C for another 3 h. The catalyst will be called PtZrGa. In a similar way, Ga/MCM-41 (Ga) and Al/MCM-41 (Al) samples were prepared. PtZrGa catalyst was pre-activated in hydrogen spiked with 50 ppm of CS_2 at 200 °C for 2 h.

2.2. Catalyst characterization

Catalysts were analyzed before and after 3 and 10 cycles under operation with the same feed and operating conditions (Fresh, Spent 1 and Spent 2).

2.2.1. X-ray

X-ray powder diffraction has been performed in a Philips PW-1830 diffractometer equipped with a graphite monochromator. The data was obtained with a 0.02° step size, using 3 s in each step and the spectra was analyzed using commercial software.

2.2.2. Chemical analysis

The concentration of C, S, Zr, Ga and Pt was determined by atomic adsorption.

2.2.3. FTIR

The IR spectroscopy of the catalyst on KBr was carried out using a Perkin-Elmer FTIR with DGS. The regions from 1600 to 1000 cm^{-1} and from 3600 to 3000 cm^{-1} were analyzed before and after adsorption of pyridine. The catalyst samples were treated in a specially designed reaction cell. There, they were degassed in vacuum at 1 Torr for 20 min and then contacted at room temperature with an argon stream containing 0.1% pyridine. After that, the cell was heated at 200 and 300 °C in argon to desorb the pyridine. The values were reported in Table 4 as μmol pyridine/g of sample.

2.2.4. ^{71}Ga NMR and ^{1}H NMR analysis

The gallium NMR spectra were obtained with a Bruker AMX-300 operating at 180 MHz. The samples were spun up to 10 kHz with air using 5 μs pulse width in a 50 ms recycle delay and 100,000 scans. GaO was used as standard internal. ^{1}H NMR hydroxyls spectra were obtained at 400.1 MHz, with the same spectrometer, with a 2 nm MAS probe and a sample spinning rate of 8 MHz and 500 scans. TMS and HFP (hexafluor-propanol) were used as reference.

2.2.5. X-ray photoelectron spectroscopy

The spectra were obtained in a Leybolh-Hereaus LHS-22 apparatus (Mg cathode) using a power of 50 eV (Ref. C_{1s}: 285.0 eV). XPS analyses have been used to assess the metal dispersion on catalysts using the peak area intensity (corrected) to measure atomic concentration. Binding energies were measured in fresh oxide catalysts. The Shirley-type background was subtracted and the Zr, Ga, Si and O species were measured by peaks deconvolution and integration to obtain the area. The signals are reported here as a ratio of metal to total metal in surface. Platinum, at the low concentration used here, was feebly detected.

2.3. Chemical reactions

The effects of the operating variables at constant temperature were obtained in a small-scale semi-batch-type reactor. This unit has a volume of 30 cm^3 that operated isothermally at 300 rpm of stirring rate. The hydrogen was added continuously to maintain the total pressure constant by an automatic pressure controller. Five samples of liquids were taken as a function of time and then analyzed using a Varian gas chromatograph, equipped with CP-Sil capillary column. The column activity was verified using a standard sample. Conversions of ethylene–propylene and the product distribution were measured in presence of 50 ppm of CS_2, hydrogen and benzene. All test used a constant benzene/olefins ratio of 1. Three different molar ratios of ethylene/propylene were employed to evaluate their effects on selectivity (ratio: 1, 2 and 3). Furthermore, three H_2 partial pressures (0.4, 0.8 and 1.2 MPa) and three temperatures (420, 430 and 440 K) were tested. A pre-activated fresh catalyst was used in each operating condition studied. Total pressure was kept constant at 1.8 MPa. In addition, another two set of tests were performed at two hydrogen partial pressure for PtGaZr and Ga catalysts, maintaining all the other operating conditions and feedstock properties constant (430 K, E/P: 2 and t: 1 h). In these tests, the catalyst was recovered after being under reaction conditions for 1 h and then reused with other fresh feed. The procedure was repeated either 3 times (Spent 1) or 10 times (Spent 2) to check the catalyst deactivation.

2.4. Set of reactions considered

The cyclization paths of reaction proceed through a first stage where the olefins are adsorbed on an ''acidic''-type center. The adsorbed species suffer electronic delocalization to produce a carbocation that reacts with a nearby adsorbed olefins to generate a C_5 and C_6 cycles or C_4–C8 n- and iso-olefins that can be desorbed or cracked back (β-scission) to

Table 1
Set of reactions (P–P)[a]

HC	HC	H_2	Products	
C_3H_6	C_3H_6	–	MeCP	$CH_3C_5H_9$
$CH_3C_5H_9$	–	–	CH	C_6H_{12}
C_6H_{12}	–	−3	B	C_6H_6
C_3H_6	C_3H_6	–	iso-$C_6^=$	C_6H_{12}
C_3H_6	C_3H_6	–	*n*-$C_6^=$	C_6H_{12}
C_6H_{12}	–	1	*n*-C_6	C_6H_{14}
C_6H_{12}	–	1	iso-C_6	C_6H_{12}
C_6H_{12}	–	2	$C_1 + C_5$	$CH_4 + C_5H_{12}$
C_6H_{12}	–	2	$C_2 + C_4$	$C_2H_6 + C_4H_{10}$

[a] Similar reactions occur for E–P, E–E, E–B and P–B.

produce lower carbon number alkenes or another carbocation ion (lighter products). It was reported that a Brönsted-type center of medium–high strength is required for this reaction. Olefins desorb (cyclic or dimeric or trimeric species) and migrate to the metal site where they are deshydrogenated, isomerized and hydrogenolyzed. Diolefins and cyclo-olefins react too fast (hydrogenation or polymerization) to be taken into account. Only traces of diolefins were found in the product as well as products higher than C_8 carbon number. For example, Table 1 shows the set of reactions considered for propylene (P)–propylene (P). The same can be considered for ethylene–ethylene and ethylene–propylene, ethylene–butene and propylene–butene. The mass transfer control for the faster reaction have been verified for the transport from the liquid to the film (k_{l-f}) and from the film to the solid (K_{f-s}) using the information measured by Tekie et al. [10]. For example, for propylene in benzene is $K_{l-f}a$: 0.01 s^{-1} and $K_{f-s}a$: 0.0017 s^{-1}. In addition, the effective diffusivity in the pores (D_{eff} 3.4 × 10^9 m^2/s) was also calculated for propylene in benzene using a tortuosity factor of 2 and porosity of 0.48. The calculus of the Dankoeler number and the Thiele module confirmed that chemical reaction control the dimerization.

3. Results

3.1. Catalysts physical properties

The catalyst has a surface area of 287 m^2/g, a pore volume of 0.48 cm^3/g, an average pore diameter of 10 nm and a particle size of 2 μm obtained directly by synthesis.

3.2. Catalyst bulk composition

The new catalyst has a ratio Si/Ga of 20 and a Si/Zr of 30 wt (see Table 2). It contains a lower amount of Pt (weight) than a commercial reforming or isomerization catalysts. Fresh catalyst does not contain carbon, while spent ones shows the accumulation of coke and sulfur as a function of the successive number of cycles in operation, which produced their deactivation (Fig. 1).

Table 2
Chemical properties of the catalysts (wt)

Catalyst	Fresh	Spent 1	Spent 2
Pt%		0.1	
ZrO_2%		2	
Ga_2O_3%		4.7	
S%	0.01	0.04/0.06*	0.07/0.09
C%	0	0.1/0.16	0.5/0.7

The XRD analysis of the sample before calcination shows the three similar peaks reported by Takeguchi [11], who assigned the regular Ga distribution in the hexagonal rod structure that grew around the surfactant, which produced large gallium dispersion. A poorly defined signal attributed to MCM-41 in the 2θ low angle region indicated some degree of amorphization in the zeolite, probably due to the Zr intercalation in the framework. This amorphization which increased during calcinations is responsible for the lower surface and higher pore diameter of the catalyst in comparison with those obtained before calcination. A no defined signal associated to cubic or monoclinic ZrO_2 was detected, but the bell shape in the background might be associated to the increases of the unit cell by the Zr and Ga intercalated species in the framework. After calcinations, the signal of Ga was also broadened and had mainly disappeared. It might indicate the Ga migration to the surface, out-of-framework. The ^{71}Ga NMR spectra of the PtZrGa samples were recorded with a large numbers of scans (Fig. 2). Before calcinations, the ^{71}Ga did not present any defined signal but after calcinations, two peaks at 150 and 15 ppm had appeared. Similar peaks have been reported by Cheng et al. [12]. The Ga in a tetrahedral coordination generated the 150 ppm while the octahedral is responsible for those at 15 ppm. A detailed study of the ^{71}Ga NMR and ^{29}Si NMR analysis is ongoing to better define the effect of calcinations temperature. It seems that tetrahedral and octahedral signals are mainly due to out-of-framework Ga species stabilized by Zr and Si. Otherwise has been reported by Takeguchi [11], who mentioned that Ga looses its tetrahedral signal (Si–O–Ga) during the calcination of the as-synthesized catalyst as a result of Ga migration to the surface, where mainly Si had been present. The presence of Zr–O in surface of the new catalyst provided the opportunity

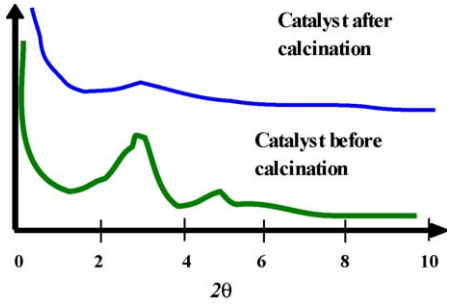

Fig. 1. DRX before and after calcinations.

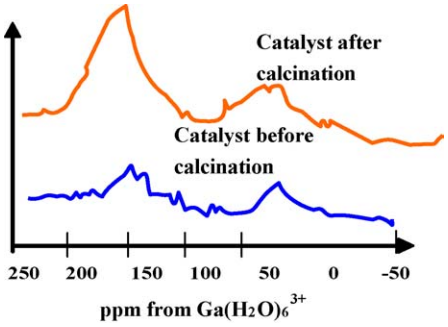

Fig. 2. Ga NMR before and after calcination.

to build the Ga–O–Zr and Ga–O–Si clusters that might "fix" the Ga well dispersed in surface.

3.3. Catalysts surface composition

XPS analysis is shown in Table 3, where the second column shows the binding energy and the third the ratio of the peak intensity for the Ga and Zr signal with respect to the intensity of Si, before and after the calcination (new catalyst). The information indicated a higher concentration of Ga^{I} in surface after calcination due to the migration of Ga from the framework. A weak signal (broad shoulder) appeared at 1115.4 eV and is attributed to the presence of Ga^{0} that might be located in the framework. Another signal present at 1120 eV is assigned to Ga^{III}. The first signal decreased while the second augmented with catalyst calcinations. The observed oxygen signal (O 1s, 533.2 eV) also enlarged after the calcination and it appeared a new signal at 531.1 eV. The last one is assigned to the bridged oxygen to Ga and Zr. It is important to notice the presence of S 2p species (102.8 eV) in surface (activate-catalyst), probably due to sulfur bounded to Pt clusters. The same analysis performed on Ga catalyst shows a more defined signal at 1115 and 1120 eV, and the absence of those of Ga^{0}, and it has a ratio I_{Me}/I_{Si} of 0.7, which indicated a lower dispersion than those measured in PtZrGa catalyst.

The FTIR spectra of the new catalyst before pyridine adsorption presents a broad band in the zone of 960 and 3742 cm^{-1} (stretching bands) [13], similar than those of pure siliceous MCM-41 that are attributed to silanol groups. Other band is present at 750 cm^{-1}, assigned to Zr–O vibrations. The PtZrGa sample still contains an important band in the 960 cm^{-1} region that increases with calcinations and is similar to those of Ti-MCM-41, reported by Blasco et al. [14], but it has lost most of the 3742 cm^{-1} band.

The ZrGa/MCM-41 surface contains various types of acid sites that may adsorb pyridine: two of them are the well known Brönsted-type attributed to the –Ga–O–Si hydroxyls on surface and the other to the –Ga–O–Zr hydroxyls (internal, in the zeolitic cage and external, out-of-framework). Both would provide a broader distribution of acid strengths. The FTIR (not shown) of the adsorbed pyridine molecule presents the typical bands of Ga–Si at 1620, 1544 and 1456 cm^{-1}, and those of Ga–Zr at 1624, 1540 and 1460 cm^{-1} [15]. The 1620–1624 bands are attributed to pyridine coordinated in Lewis sites Ga^{3+}. Those bands at 1540–1544 are due to Brönsted acid sites. The catalyst also presents small bands at 1550, 1500 and 1680 cm^{-1} that are similar to those reported for Al-MCM-41, indicating a more complex pattern of Ga interactions with the surface of the zeolite than those observed on Ga/AlZSM-5 [16].

Table 4 depicted the amount of pyridine that remains adsorbed at 200 and 300 °C in the Brönsted-type site (1540–1544 cm^{-1}) and in the Lewis-type site (1450 cm^{-1}) on calcinated catalyst. The analysis is compared with those observed for the Ga and Al catalysts (ratios of Si/Ga and Si/Al: 20). It can be seen that PtZrGa presents at 200 °C, intermediate Brönsted and Lewis acidity than Ga and Al samples. PtZrGa is interesting for keeping most of the Lewis acidity at 300 °C and for having the highest L/B ratio of all. Also, the PtGaZr and Ga samples might have some basic sites as measured by Petre et al. [15] for Ga/MCM-41.

The proton NMR analysis of the hydroxyls is strongly affected by the Pt attenuation. The qualitative analysis indicated the presence of one small peak at 1.7 (attributed to the silanol group of the MCM-41) and a shoulder between 2 and 5 ppm. A similar signal was reported by Fang et al. [13] for Ga/MCM-41 and here is attributed to silanol groups of Ga–Si and Ga–Zr species.

Finally, a preliminary TEM analysis indicated the absence of a cluster bigger than 1 nm on surface.

3.4. Effect of reaction time and temperature

The catalyst was tested at constant ratio of benzene to olefins (B/E), while changing the ethylene/propylene ratio (E/P), the temperature and the hydrogen partial pressure. Fig. 3 shows as an example the conversion of ethylene as a function of reaction time and temperature for E/P ratio of 2 and p_{H_2}: 0.8. The figure indicates a relative low sensibility of the ethylene conversion to the reaction temperatures.

The reaction products are divided into two groups of components: the aromatics (Ar) and cyclo-paraffins (CP) on

Table 3
XPS analysis (before/after calcination)

Metal	Binding energy (eV)	I_{Me}/I_{SiO_2}
Ga	1183 $2p_{3/2}$	1/1.5
Zr	182 $3p_{3/2}$	0.4/0.9
Si	103.4 2p	–

Table 4
Pyridine adsorption (FTIR) PtGaZr

	Temperature (°C)	
	200	300
B (1454 cm^{-1})	1.1/0.2/1.8	0.5/0/0.9
L (1540 cm^{-1})	2.8/3.1/0.7	2.1/0.7/0.4

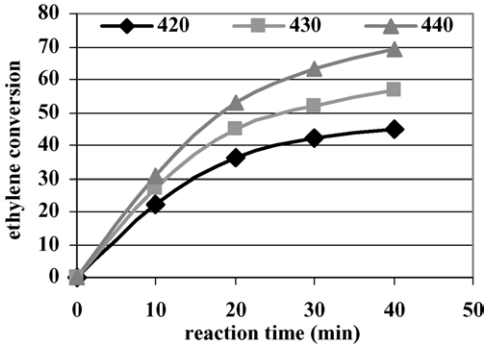

Fig. 3. Conversion of ethylene.

one hand and the iso- and *n*-paraffins (P) on the other. The production of the first two is shown in Fig. 4 for 50% ethylene conversion, E/P ratio of 2 and p_{H_2}:10 MPa. The third and fourth ones are presented in Figs. 5 (below) for the same conditions. Fig. 4 shows the high selectivity of the catalyst towards the benzene production, as well as the presence of the cyclo-paraffins intermediaries. The higher the temperature, the higher is the production of aromatics and the lower are the paraffins and cyclo-paraffins generated. Fig. 5 indicates that the production of C_4–C_5 iso-paraffins was favored in comparison with *n*-paraffins. At same level of conversion, the effect of increasing temperatures goes in direction to increase is selectivity toward the C_4–C_5 paraffin production. It was observed that the amount of coke on catalyst after three cycles augmented with temperature, but the sulfur content remained constant.

The paraffins are produced by hydrogenation and cracking of olefins. When the temperature is raised, the C_4 paraffins are slightly reduced while C_5–C_7 paraffins are notably decreased, being the reduction higher for *n*-paraffins than for iso-paraffins. Only small amounts of propane were found in the product probably because although they might be formed, they were converted into aromatics.

3.5. Effect of hydrogen partial pressure

The ethylene conversion is not affected by doubling the hydrogen partial pressure but the aromatic and cyclo-paraffin production are reduced as well the catalyst

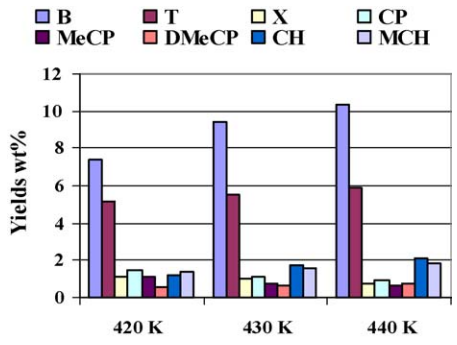

Fig. 4. Aromatics production.

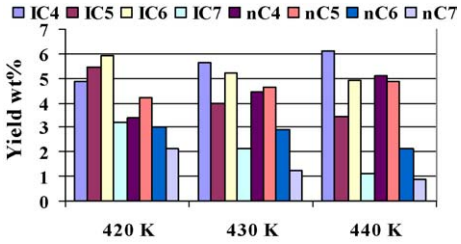

Fig. 5. Paraffins production.

deactivation. Fig. 6 shows the results of operating at 0.8 or 1.4 MPa, 440 K and E/B: 2, for the catalyst that had undertaken either 3 or 10 tests. A decline in activity can be observed as a consequence of coke accumulation on the surface (see coke content in Table 4) giving place to a decrease in acidity. Choudhary et al. [17] had concluded—for the propane aromatization on Ga containing catalyst—that the activity and selectivity as well as the catalyst deactivation were proportional to the total acidity measured, for example, in terms of pyridine chemisorbed. The coke produced the dehydrogenation to cracking ratio and the aromatics to methane + ethane mass ratio in the products are expected to increase proportionally to initial acidity. The main problem observed regarding Ga catalyst is that a very active and selective catalyst for olefins to aromatic conversion deactivates very fast. Costa et al. [4] had reported similar behavior with ethylene–propylene for NaY zeolite. However, we found a better PtZrGa selectivity towards aromatics and lower rate of coke forming than for Ga catalyst. The former has lower deactivation than the latter. It is important to remember that the new catalyst has a quite similar total initial pyridine acidity than Ga, but a completely different B/L acidity (Ga < GaZr).

The new catalyst produced less amount of coke than those based on Ga or Al due to the ability of Pt to hydrogenated the intermediaries, the use of a lower operating temperatures (less than 30 °C) for the same olefins conversion and to the presence of adsorbed benzene on surface. The last two factors limit the cracking reactions. The results shown in Fig. 6 indicate that after having an initial important deactivation (three cycles), the posterior rate of deactivation is reduced at similar total conversion. It seems that coke is initially accumulated on the strongest acid sites, which have

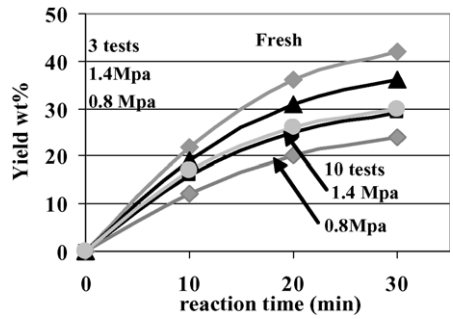

Fig. 6. Effect of hydrogen partial pressure in deactivation (3 tests: Spent 1; 10 tests: Spent 2).

Table 5
Selectivity of deactivated catalysts

	Catalyst			
	PtGaZr		Ga	
	Ar/CH_4[a]	Ar/par.[a]	Ar/CH_4[a]	Ar/par.[a]
Fresh	5.0/6.1	10.2/10.6	10/–	15/–
Spent 1	4.7/5.4	9.8/10.7	8/–	9/–
Spent 2	4.3/5.0	9.4/10.8	6/–	5/–

[a] Represent ratios.

a limited participation in the main reactions. The higher the p_{H_2}, the lower is the deactivation. Table 5 shows the ratios aromatics to methane + ethane and aromatics to paraffins for PtGaZr and Ga at 0.8 MPa (left side column) and 1.4 MPa (right side column) of hydrogen partial pressure. The operating conditions were 420 K, 20 m, E/P: 2.

The lower amount of coke formed in PtZrGa compared to Ga explains the lower reduction in aromatics/paraffins ratio produced for the same ethylene conversion and time of reaction. The effect of hydrogen partial pressure was only observed in PtGaZr catalyst, due to its Pt content, in spite of that, some degree of sulfiding might have also affected the new catalyst. Pt is known for its ability to dehydrogenate faster than Ga, reducing the possibility for the nearby olefins to proceed into aromatic or coke formation and in this way, iso- or normal olefins might desorb from the acid sites to be hydrogenated without aromatization. That reduces the aromatics production but keeps the acid sites ''cleaner''. The optimal hydrogen pressure is a tried-off selection: either deactivated or loss of some aromatic production.

3.6. Effect of E/P ratio

Ethylene/propylene ratio affects both the reactivity and selectivity. Higher the ratio, lower is the rate of olefins conversion and the molecular weight of the products. No particular effect of this ratio and the hydrogen partial pressure were observed on the catalyst deactivation rate or coke on the catalyst.

3.7. Mechanism of ethylene and propylene oligomerization

The olefins oligomerization produces a broad range of aromatics, paraffins and iso-paraffins. The mechanism for propane butanes aromatization on Ga/zeolite has been discussed by us [6] and by Guisnet and Gnep [18], among others. We proposed ethane and propane activation via dehydrogenation in Ga and the migration of the olefins to the acid sites, where they proceed with the oligomerization, cyclization and cracking reactions through a complex mixture of insaturated intermediaries. For propane and using Ga catalyst with medium operating temperature (500–600 K), the limiting step is the olefins formation. With PtZrGa and performing the reaction at lower operating temperature (420–440 K), the limiting step is the olefins oligomerization to cyclo-alkenes. The olefins are adsorbed in a Ga–O–Si or Ga–O–Zr acid site where they form a adsorbed carbanion–carbocation, while other is adsorbed in a nearby acid sites to form other carbanion–carbocation that might interact via dipole–dipole and form a larger adsorbed dipole. If this dipole is located in a hexagonal or pentagonal structure, the cycle could be closed and desorbs or form larger olefins. The new catalysts has Pt and a large proportion of Lewis acid sites than Brönsted one and may adsorb the olefin trough sigma and pi interaction.

The isomerization and cracking of these adsorbed large molecules that are formed and then destroyed produce a series of di- and tri-branched olefinic intermediaries ($iC_5^=$, $iC_6^=$, $iC_7^=$). They are responsible for the generation of C_1–C_2 and smaller iso- and *n*-paraffins. Isotopic studies performed by Biscardi and Iglesia [19] with ^{13}C propane molecules indicated the presence of some of the intermediaries that we propose here for the olefins dimerization (Table 1).

3.8. Industrial implications

The valorization of DC and FCC light olefins can be done by using a PtZrGa/MCM-41-type catalyst. In spite of catalyst, deactivation could be controlled by employing hydrogen, aromatics and CS_2 in liquid phase, an adequate reactor system with continuous catalyst replacement and regeneration that will be mandatory. All of them will impact the economy for a commercial application. Additional work is still needed to solve these challenging constraints.

4. Conclusion

Olefins can be converted into aromatics and cyclo-paraffins by dimerization–oligomerization of ethylene and propylene in presence of CS_2, hydrogen and benzene using a PtGaZr/MCM-41 catalyst. The following was observed in the study:

- The catalyst has a bifunctional active surface composed by a metal site (Pt) and by complex acid sites (Ga–O–Zr and Ga–O–Si).
- The main products obtained with this catalyst are aromatics and iso-paraffins. The product distribution changes with the E/P ratio, temperature and reaction time, but always benzene and iC_4, iC_5, paraffins are the major products. Higher the temperature and reaction time, higher is the amount of methane and coke formed.
- The catalyst initially deactivated relatively fast but then the rate of deactivation decreased. The higher the hydrogen partial pressure, the lower is the coke formed and better is the selectivity to benzene.
- The surface of the catalyst has a higher proportion of Lewis than Brönsted sites than Ga/MCM-41, probably associated to the Ga–O–Zr and Ga–O–Si clusters. The Ga and Zr are located in and out-of-framework. Additional

effort needs to be made to control the acid sites in order to reduce the catalyst deactivation.

Acknowledgments

The authors want to thank Dr. J. Reverse for the ^{17}Ga NMR analysis and the economical support of Simon Bolivar University.

References

[1] T. Xie, K.B. Mc Auley, J.C.C. Hsu, D.W. Bacon, Ind. Eng. Chem. Res. 33 (1994) 449–479.
[2] M. Golombock, J. de Brujin, Ind. Eng. Chem. Res. 39 (2000) 267–271.
[3] R. Galiasso Tailleur, Platin JB, US Patent Pending, 2004.
[4] C. Costa, J.M. Lopes, F. Lemos, F. Ramoa Rivero, J. Mol. Catal. A Chem. 144 (1999) 207–220.
[5] L. Johnson, C.H.M. Killian, M. Brookart, J. Am. Chem. Soc. 117 (1995) 6414–6415.
[6] G. Giannetto, R. Monque, R. Galiasso Tailleur, Catal. Rev. 36 (2) (1994) 271–304.
[7] J.R. Mowry, J.D.C. Martindale, A.P.H. Hall, Arabian J. Sci. Eng. 10 (1985) 367–375.
[8] C.T. Kresge, M.E. Leonowicz, W.J. Roth, J.C. Vartulli, US Patent No. 5,098,684 (1992).
[10] J.L.Z. Tekie, T.I. Mizan, B.I. Morsi, E.E. Maier, C.P.P. Sigh, Chem. Eng. Sci. 4 (2004) 549–559.
[11] T. Takeguchi, J.B. Kim, M. Kang, T. Inui, W.T. Cheuh, J. Catal. 175 (1998) 1–6.
[12] C. Cheng, H. He, W. Zou, J. Klinoski, J.A. Goncalvez, L.F. Gladden, J. Phys. Chem. 100 (1996) 390–397.
[13] K. Fang, J. Ren, Y. Sun, J. Mol. Catal. A Chem. 229 (2005) 51–58.
[14] T. Blasco, A. Corma, M.T. Navarro, J. Perez-Pariente, J. Catal. 156 (1995) 65–74.
[15] A.L. Petre, A. Auroux, P. Gelin, M. Caldararu, N.I. Ionescu, Thermochim. Acta 379 (2001) 177–185.
[16] Z. Gabelica, C. Mayenez, R. Monque, R. Galiasso Tailleur, G. Giannetto, Molecular Sieves, Van Reinhold, NY, 1992 (Chapter 15-Ed, vol. 1, pp. 190–221).
[17] V.R. Choudhary, P. Devadas, A.K. Kinage, M. Guisnet, Zeolites 18 (2–3) (1997) 188–195.
[18] M. Guisnet, N.S. Gnep, Appl. Catal. A Gen. 146 (1996) 33–34.
[19] J.A. Biscardi, E. Iglesia, Catal. Today 31 (1996) 207–231.